

Article

# Assessing Effect of Targeting Reduction of PM<sub>2.5</sub> Concentration on Human Exposure and Health Burden in Hong Kong Using Satellite Observation

Changqing Lin <sup>1,2</sup>, Alexis K. H. Lau <sup>1,2</sup>, Xingcheng Lu <sup>2</sup>, Jimmy C. H. Fung <sup>2,3</sup>, Zhiyuan Li <sup>2</sup>, Chengcai Li <sup>4</sup> and Andromeda H. S. Wong <sup>2,\*</sup>

<sup>1</sup> Department of Civil and Environmental Engineering, The Hong Kong University of Science and Technology, Hong Kong 999077, China; cqlin@ust.hk (C.L.); alau@ust.hk (A.K.H.L.)

<sup>2</sup> Division of Environment and Sustainability, The Hong Kong University of Science and Technology, Hong Kong 999077, China; xclu@ust.hk (X.L.); majfung@ust.hk (J.C.H.F.); zliar@ust.hk (Z.L.)

<sup>3</sup> Department of Mathematics, The Hong Kong University of Science and Technology, Hong Kong 999077, China

<sup>4</sup> Department of Atmospheric and Oceanic Sciences, School of Physics, Peking University, Beijing 100871, China; ccli@pku.edu.cn

\* Correspondence: ahs Wong@ust.hk; Tel.: +86-(852)-2358-6676

Received: 14 October 2018; Accepted: 5 December 2018; Published: 19 December 2018



**Abstract:** Targeting reduction of PM<sub>2.5</sub> concentration lessens population exposure level and health burden more effectively than uniform reduction does. Quantitative assessment of effect of the targeting reduction is limited because of the lack of spatially explicit PM<sub>2.5</sub> data. This study aimed to investigate extent of exposure and health benefits resulting from the targeting reduction of PM<sub>2.5</sub> concentration. We took advantage of satellite observations to characterize spatial distribution of PM<sub>2.5</sub> concentration at a resolution of 1 km. Using Hong Kong of China as the study region (804 satellite's pixels covering its residential areas), human exposure level ( $c_p$ ) and premature mortality attributable to PM<sub>2.5</sub> (*Mort*) for 2015 were estimated to be 25.9  $\mu\text{g}/\text{m}^3$  and 4112 people per year, respectively. We then performed 804 diagnostic tests that reduced PM<sub>2.5</sub> concentrations by  $-1 \mu\text{g}/\text{m}^3$  in different areas and a reference test that uniformly spread the  $-1 \mu\text{g}/\text{m}^3$ . We used a benefit rate from targeting reduction (BRT), which represented a ratio of declines in  $c_p$  (or *Mort*) with and without the targeting reduction, to quantify the extent of benefits. The diagnostic tests estimated the BRT levels for both human exposure and premature mortality to be 4.3 over Hong Kong. It indicates that the declines in human exposure and premature mortality quadrupled with a targeting reduction of PM<sub>2.5</sub> concentration over Hong Kong. The BRT values for districts of Hong Kong could be as high as 5.6 and they were positively correlated to their spatial variabilities in population density. Our results underscore the substantial exposure and health benefits from the targeting reduction of PM<sub>2.5</sub> concentration. To better protect public health in Hong Kong, super-regional and regional cooperation are essential. Meanwhile, local environmental policy is suggested to aim at reducing anthropogenic emissions from mobile and area (e.g., residential) sources in central and northwestern areas.

**Keywords:** PM<sub>2.5</sub>; satellite remote sensing; public health; environmental policy; Hong Kong

## 1. Introduction

Epidemiological studies have shown that long-term exposure to PM<sub>2.5</sub> (particulate matter with an aerodynamic diameter of less than 2.5  $\mu\text{m}$ ) is associated with a range of adverse health issues [1–6]. High levels of exposure to PM<sub>2.5</sub> have been extensively documented around the world [7–9]. Global population-weighted mean PM<sub>2.5</sub> concentration from 2001 to 2010 was estimated to be 26.4  $\mu\text{g}/\text{m}^3$ ,

which substantially exceeded the World Health Organization (WHO) air quality guideline (AQG,  $10 \mu\text{g}/\text{m}^3$ ) [10]. Several health impact assessments showed that about 3.2 million premature deaths were attributable to  $\text{PM}_{2.5}$  around the world and most of them occurred in low- and middle-income countries [11,12].

China has experienced a rapid economic growth and urbanization within the past few decades, resulting in severe air pollutions from  $\text{PM}_{2.5}$  [13]. Hong Kong, one of the most populous cities in the world, is a special administrative region of China. It locates in southeast of the Pearl River Delta (PRD) region, which has been recognized as one of the largest city groups in the world [14]. Air quality in Hong Kong is greatly determined by local emissions and regional transports from mainland China [15,16]. In common with other Chinese cities,  $\text{PM}_{2.5}$  concentration in Hong Kong is much higher than in most cities in Europe and North America [17,18]. The population-weighted mean  $\text{PM}_{2.5}$  concentration in Hong Kong from 2000 to 2014 was estimated to be  $32.5 \mu\text{g}/\text{m}^3$  [8]. Liao et al. [19] estimated the annual premature mortality attributable to  $\text{PM}_{2.5}$  exposure to be 2918 people per year for Hong Kong from 2001 to 2016. Using satellite observations, Lu et al. [20] showed that the annual premature death attributable to  $\text{PM}_{2.5}$  over Hong Kong ranged from 4900 to 5700 people per year from 2004 to 2013.

Spatiotemporal variations in  $\text{PM}_{2.5}$  concentration have been traditionally characterized using fixed-site observations [21]. Such monitoring, however, is difficult to cover entire region and fully delineate the spatial distribution of  $\text{PM}_{2.5}$  concentration [22]. To reduce population exposure level and better protect public health, reducing  $\text{PM}_{2.5}$  concentration level is an intuitive suggestion for environmental policies [23,24]. Targeting reduction of  $\text{PM}_{2.5}$  concentration lessens population exposure level and health burden more effectively than uniform reduction does. The lack of spatially explicit  $\text{PM}_{2.5}$  data limits quantitative assessment of the effect of targeting reduction, particularly in the developing countries.

This study aims to investigate extent of exposure and health benefits resulting from the targeting reduction of  $\text{PM}_{2.5}$  concentration. We use Hong Kong of China as the study region. Although  $\text{PM}_{2.5}$  concentrations have been regularly monitored at sixteen stations over Hong Kong, these ground monitors still cannot fully cover the entire region. Satellite remote sensing provides an important alternative method toward filling the spatial gap left by fixed-site observations [25–28]. In this study, we take advantage of high-resolution satellite observations to characterize the spatial variation in  $\text{PM}_{2.5}$  concentration over Hong Kong. We then investigate the extent of exposure and health benefits if  $\text{PM}_{2.5}$  reduction targets the population hotspots. Finally, implication for local environmental policy is discussed.

## 2. Materials

### 2.1. Population Density

The census provides systematic population data by administrative regions. However, the spatial matching of the census data and the gridded pollution data is difficult. Using gridded population data derived from a spatialization of the census data is an effective method to solve this issue. We obtained gridded data of yearly average of population density for 2015 from the LandScan database (<http://web.ornl.gov/sci/landscan/>). The LandScan population data are developed by the Oak Ridge National Laboratory [29]. The LandScan algorithm uses best available census and geographic data (e.g., land use, roads and village locations) and remote sensing imagery analysis techniques to disaggregate census counts within administrative boundaries. Based upon the spatial data and the socioeconomic and cultural understanding of an area, the possible occurrence of population during a day is taken into account. The resultant population count is an ambient population density (average over 24 h including day and night). The LandScan population data show valuable applications in environmental, social and economic studies [30–32]. The LandScan data estimated total population of Hong Kong for 2015 to be 7.06 million, which was lower than that derived from the census

(7.29 million) by 3.2%. We obtained district-level population data of Hong Kong from the population census (<https://www.censtatd.gov.hk/hkstat/sub>). The LandScan population data were then adjusted by district-level factors to match the census's populations.

Figure 1a shows spatial distribution of population density ( $\rho$ ) at a resolution of 1 km over Hong Kong. Eighteen districts of Hong Kong are marked. Consistent spatial pattern was seen between the LandScan- and census-based population data [33]. Low population densities were seen in some highly rural areas of Hong Kong. In this study, we took into account only residential areas with a population density of  $\geq 10$  people/km<sup>2</sup>. These residential areas over Hong Kong contained 804 satellite's pixels. Mean population density ( $\rho_0$ ) over the residential areas of Hong Kong was about 8978 people/km<sup>2</sup>.

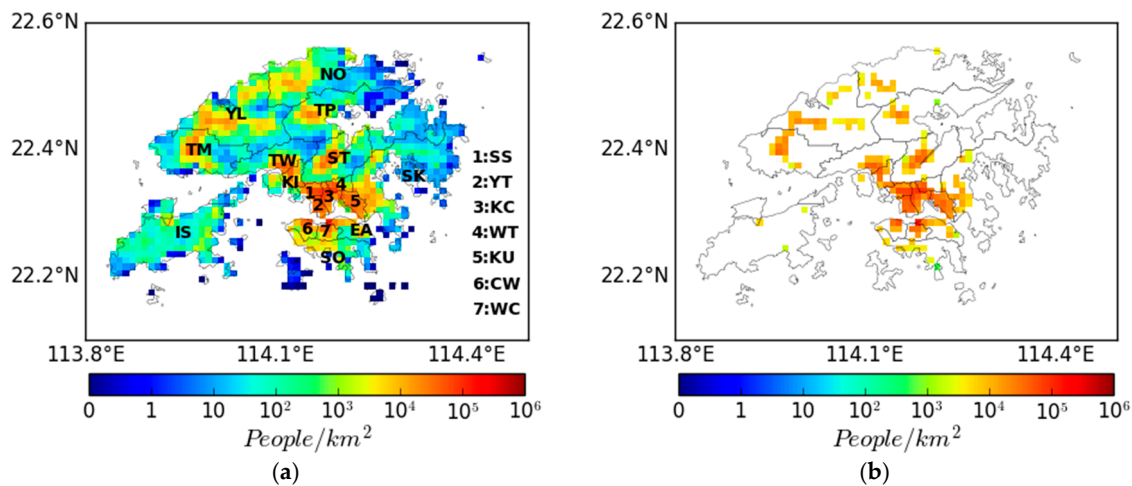


**Figure 1.** (a) Spatial distribution of population density ( $\rho$ ) at a resolution of 1 km over Hong Kong. Eighteen districts of Hong Kong [Sham Shui Po (SS), Yau Tsim Mong (YT), Kowloon City (KC), Wong Tai Sin (WT), Kwun Tong (KU), Central & Western (CW), Wan Chai (WC), Eastern (EA), Southern (SO), Kwai Tsing (KI), Tsuen Wan (TW), Sha Tin (ST), Sai Kung (SK), Tai Po (TP), Tuen Mun (TM), Yuen Long (YL), North (NO) and Islands (IL)] are marked. (b) Population density in the more populated areas of Hong Kong.

We classified the residential areas into more populated areas ( $\rho \geq \rho_0$ ) and less populated areas ( $\rho < \rho_0$ ). Mean population densities (38,872 and 1022 people/km<sup>2</sup>) differed greatly between the two areas. Figure 1b shows population density in the more populated areas of Hong Kong. These areas accounted for 21% (169 pixels) of the residential areas. Most of them were located in central and northwestern areas of Hong Kong.

## 2.2. Satellite-Derived PM<sub>2.5</sub>

To characterize the PM<sub>2.5</sub> variation covering all of Hong Kong, we took advantage of the technique of satellite remote sensing. The aerosol optical depth (AOD) dataset at a resolution of 1 km was constructed using spectral data from the two Moderate Resolution Imaging Spectroradiometer (MODIS) instruments aboard the Terra and Aqua satellites [34]. Then, ground-level PM<sub>2.5</sub> concentrations were derived from the AOD using an observational data-driven algorithm, which took the ground-observed visibility and relative humidity data as inputs [35,36]. We obtained annual average of satellite-retrieved PM<sub>2.5</sub> concentration data over Hong Kong for 2015 (<http://envf.ust.hk/dataview/aod2pm/current>). More details on retrieval algorithm and data evaluation were described in previous studies [35,36]. Figure 2a shows spatial distribution of the satellite-derived PM<sub>2.5</sub> concentration ( $c$ ) at a resolution of 1 km in the residential areas of Hong Kong in 2015. The points represent ground observations at 12 general stations. Much higher PM<sub>2.5</sub> concentrations occurred in the central and northwestern areas. Figure 2b shows an evaluation of the satellite-derived PM<sub>2.5</sub> concentration against the ground observations. A high correlation coefficient of 0.9 ( $N = 12$ ) was found. Root mean square error,

mean absolute error and mean absolute percentage error were estimated to be  $1.1 \mu\text{g}/\text{m}^3$ ,  $1.0 \mu\text{g}/\text{m}^3$  and 3.9%, respectively.

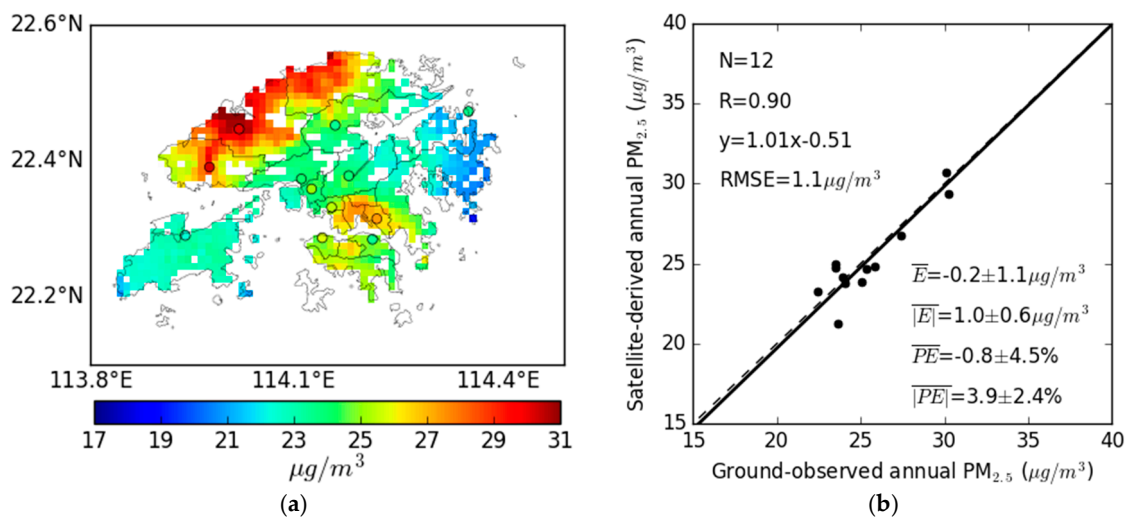


**Figure 2.** (a) Spatial distribution of the satellite-derived  $\text{PM}_{2.5}$  concentration at a resolution of 1 km in the residential areas of Hong Kong in 2015. The points represent ground observations at 12 general stations. (b) Evaluation of the satellite-derived  $\text{PM}_{2.5}$  concentration against the ground observations.

### 3. Methodology

Estimating human exposure to  $\text{PM}_{2.5}$  requires population and pollution data. In each pixel ( $i$  and  $j$ , where  $i$  ranges from 1 to  $X$  and  $j$  ranges from 1 to  $Y$ ) over Hong Kong, we denote  $\text{PM}_{2.5}$  concentration as  $c_{i,j}$  and population density as  $\rho_{i,j}$ . The population-weighted mean  $\text{PM}_{2.5}$  concentration ( $c_\rho$ ) for Hong Kong can be quantified by

$$c_\rho = \frac{\sum_{i=1}^X \sum_{j=1}^Y c_{i,j} \rho_{i,j}}{\sum_{i=1}^X \sum_{j=1}^Y \rho_{i,j}} \quad (1)$$

We estimate the premature mortality attributable to  $\text{PM}_{2.5}$  following the Global Burden Disease (GBD) study [11]. We take into account premature mortalities attributable to ambient  $\text{PM}_{2.5}$  for four major disease endpoints [stroke, ischemic heart disease (IHD), chronic obstructive pulmonary disease (COPD) and lung cancer (LC)] for adults (age  $\geq 25$ ) in Hong Kong. The premature mortality attributable to  $\text{PM}_{2.5}$  can be quantified by

$$\text{Mort}_{i,j,d,a} = I_{d,a} \cdot \frac{RR_{i,j,d,a} - 1}{RR_{i,j,d,a}} \cdot \rho_{i,j,a} \quad (2)$$

where  $I$  is reported mortality rate;  $RR$  is relative risk of premature mortality attributable to  $\text{PM}_{2.5}$  exposure. Indices  $d$  and  $a$  represent the disease endpoints and age groups, respectively. The disease- and age-specific mortality rates ( $I_{d,a}$ ) in Hong Kong for 2015 were obtained from the dataset of the GBD study (<http://ghdx.healthdata.org/gbd-results-tool>). We employed the integrated exposure-response functions (IERs) to estimate mean and 95% confidential intervals (CI) of  $RR$  attributable to  $\text{PM}_{2.5}$  exposure for different disease endpoints and age groups [37]:

$$RR = 1 + \alpha [1 - \exp(-\gamma(c - c_0)^\delta)] \text{ for } c > c_0 \quad (3a)$$

$$RR = 1 \text{ for } c \leq c_0 \quad (3b)$$

where parameters  $\alpha$ ,  $\gamma$  and  $\delta$  determine the overall shape of the concentration-response relationship as the result of a stochastic fitting process; and  $c_0$  is the counterfactual concentration below which no additional health risk is assumed. These IERs constrain the shape of concentration-response

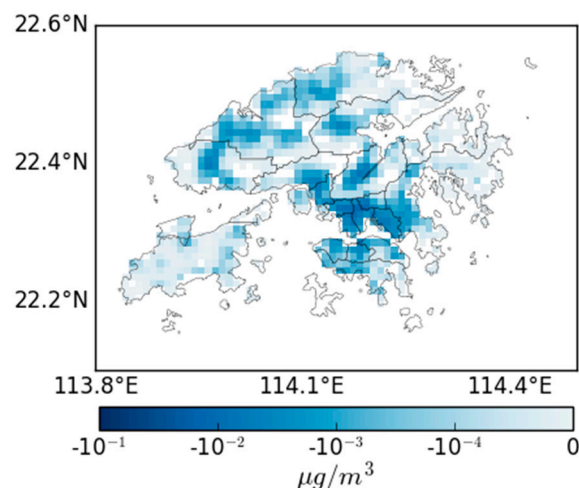
function using data for high  $PM_{2.5}$  concentrations and have been extensively applied in health impact assessments in different parts of the world [11]. The term  $(RR-1)/RR$  is attributable factor that represents the fraction of mortality attributable to  $PM_{2.5}$  exposure.  $Mort_{i,j,d,a}$  represents the disease- and age-specific premature deaths attributable to  $PM_{2.5}$  in each pixel  $(i, j)$ . Total premature mortality attributable to  $PM_{2.5}$  ( $Mort$ ) for Hong Kong is quantified by summing over premature deaths from all disease endpoints in all pixels.

Reduction of  $PM_{2.5}$  concentration in different areas of Hong Kong results in different benefits in reducing its  $c_\rho$  and  $Mort$ . We perform 804 diagnostic tests that reduce  $PM_{2.5}$  concentration by  $-1 \mu\text{g}/\text{m}^3$  in different pixels over Hong Kong. We then investigate the differences in the declines in the  $c_\rho$  and  $Mort$  levels among these tests. We also perform a reference test, in which the  $-1 \mu\text{g}/\text{m}^3$  is uniformly spread within Hong Kong. In this reference test,  $PM_{2.5}$  concentrations are uniformly reduced by  $-0.00124$  (i.e.,  $1/804$ )  $\mu\text{g}/\text{m}^3$  in all pixels. As expected, the  $c_\rho$  level of Hong Kong also reduces by  $-0.00124 \mu\text{g}/\text{m}^3$  in the reference test. In summary, we perform 804 diagnostic tests that reduce  $PM_{2.5}$  concentrations in different areas of Hong Kong and a reference test that uniformly spreads the  $-1 \mu\text{g}/\text{m}^3$ . Then, we assess the exposure and health benefits from the targeting reduction of  $PM_{2.5}$  concentration.

## 4. Results

### 4.1. Effect of Targeting Reduction on Human Exposure in HK

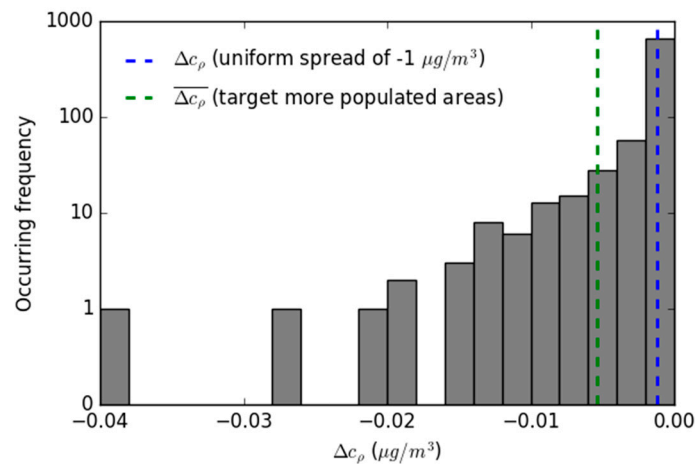
The population-weighted mean  $PM_{2.5}$  concentration ( $c_\rho$ ) for Hong Kong was estimated to be  $25.9 \pm 1.9 \mu\text{g}/\text{m}^3$  for 2015. This  $c_\rho$  level still exceeded the WHO Interim Target 2 (IT-2,  $25 \mu\text{g}/\text{m}^3$ ), IT-3 ( $15 \mu\text{g}/\text{m}^3$ ) and AQG ( $10 \mu\text{g}/\text{m}^3$ ). After we performed 804 tests that reduced  $PM_{2.5}$  concentration by  $-1 \mu\text{g}/\text{m}^3$  in different pixels, Figure 3 shows spatial distribution of the reduction of the  $c_\rho$  level of Hong Kong ( $\Delta c_\rho$ ) for these tests. The  $c_\rho$  levels experienced a greater reduction when reducing  $PM_{2.5}$  concentration in more populated areas (e.g., central and northwestern areas). The most substantial reduction of  $c_\rho$  was about  $-0.039 \mu\text{g}/\text{m}^3$  when reducing  $PM_{2.5}$  concentration by  $-1 \mu\text{g}/\text{m}^3$  in central urban areas.



**Figure 3.** Spatial distribution of the reduction of the  $c_\rho$  level of Hong Kong ( $\Delta c_\rho$ ) in the 804 tests that reduced  $PM_{2.5}$  concentration by  $-1 \mu\text{g}/\text{m}^3$  in different pixels.

Figure 4 shows frequency distribution of  $\Delta c_\rho$  of Hong Kong among the 804 tests. The reduction of the  $c_\rho$  value ranged from  $-0.002$  to  $0 \mu\text{g}/\text{m}^3$  in most tests (668 out of 804). In the reference test (i.e., uniformly reduced  $PM_{2.5}$  concentration),  $c_\rho$  reduced by  $-0.00124 \mu\text{g}/\text{m}^3$  (shown by the blue-dashed line). When  $PM_{2.5}$  reduction targeted the more populated areas ( $\rho \geq \rho_0$ ),  $c_\rho$  reduced by  $-0.00539 \mu\text{g}/\text{m}^3$  on average (shown by the green-dashed line). We use a benefit rate from targeting

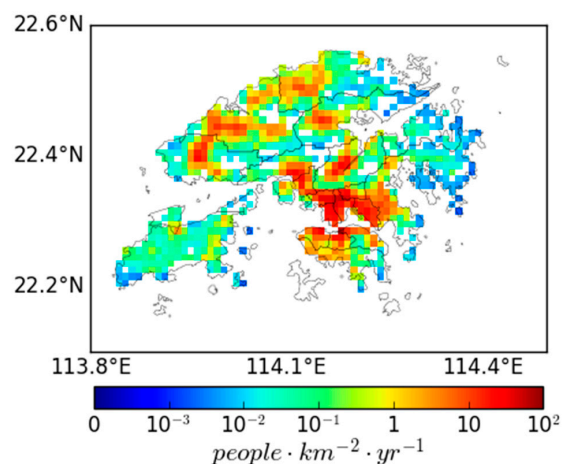
reduction (BRT), defined as a ratio of mean  $\Delta c_p$  when PM<sub>2.5</sub> reduction targets the more populated areas and  $\Delta c_p$  when uniformly reducing PM<sub>2.5</sub> concentration, to quantify the extent of benefit resulting from the targeting reduction. The BRT for exposure was estimated to be 4.33 for Hong Kong. It indicates that PM<sub>2.5</sub> reduction targeting more populous areas lessens >4 times as many human exposure as uniform reduction does.



**Figure 4.** Frequency distribution of  $\Delta c_p$  of Hong Kong among the 804 tests. The blue-dashed line represents  $\Delta c_p$  when uniformly reducing PM<sub>2.5</sub> concentration. The green-dashed line shows mean  $\Delta c_p$  when PM<sub>2.5</sub> reduction targets more populated areas.

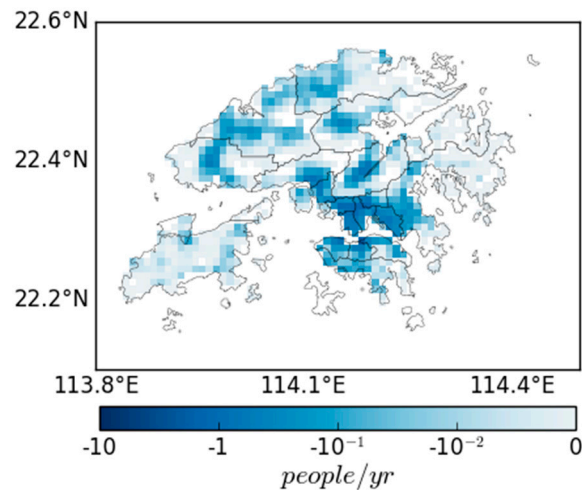
#### 4.2. Effect of Targeting Reduction on Health Burden in HK

We estimated annual premature mortality attributable to PM<sub>2.5</sub> from the four health endpoints (i.e., IHD, stroke, LC and COPD) for adults over Hong Kong in 2015. Figure 5 shows spatial distribution of the density of annual premature mortality attributable to PM<sub>2.5</sub> over Hong Kong in 2015. The highest density of annual PM<sub>2.5</sub>-attributable mortality was about 160 people·km<sup>-2</sup>·yr<sup>-1</sup> in central urban areas. Annual premature mortality attributable to PM<sub>2.5</sub> for entire Hong Kong (*Mort*) was estimated to be 4112 (95% CI: 1937, 6258) people per year. This mortality number is comparable to those from other studies [19,20]. Among the four diseases, IHD, stroke, LC and COPD resulted in 1667 (95% CI: 783, 2523), 1536 (95% CI: 721, 2350), 596 (95% CI: 286, 906) and 313 (95% CI: 147, 479) deaths per year, respectively. Therefore, IHD (40.5%) and stroke (37.4%) contributed to most of the premature mortality, while LC (14.5%) and COPD (7.6%) contributed to the remainder.



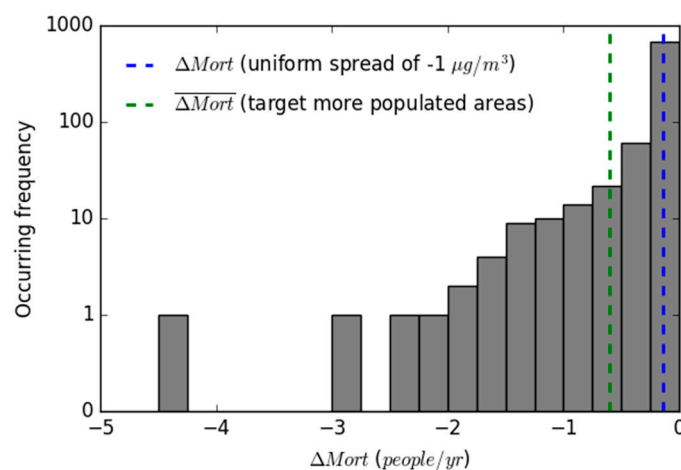
**Figure 5.** Spatial distribution of the density of annual premature mortality attributable to PM<sub>2.5</sub> for adults over Hong Kong in 2015.

Figure 6 shows spatial distribution of the reduction of premature mortality attributable to  $PM_{2.5}$  over Hong Kong ( $\Delta Mort$ ) in the 804 tests that reduced  $PM_{2.5}$  concentration by  $-1 \mu g/m^3$  in different pixels. The  $Mort$  level experienced a greater reduction when reducing  $PM_{2.5}$  concentration in central and northwestern areas. The most substantial  $\Delta Mort$  was about  $-4.39$  people per year in the test that reduced  $PM_{2.5}$  concentration in central urban areas.



**Figure 6.** Spatial distribution of the reduction of premature mortality attributable to  $PM_{2.5}$  over Hong Kong ( $\Delta Mort$ ) in the 804 tests that reduced  $PM_{2.5}$  concentration by  $-1 \mu g/m^3$  in different pixels.

Figure 7 shows frequency distribution of  $\Delta Mort$  of Hong Kong among the 804 tests. The frequency distribution of  $\Delta Mort$  shared a similar shape to  $\Delta c_p$ . The reduction of the  $Mort$  value ranged from  $-0.25$  to  $0$  people per year in most tests (679 out of 804). In the reference test,  $Mort$  reduced by  $-0.138$  people per year (shown by the blue-dashed line). When  $PM_{2.5}$  reduction targeted the more populated areas,  $Mort$  reduced by  $-0.599$  people per year on average (shown by the green-dashed line). The BRT for mortality was estimated to be 4.34, which was similar to the BRT for exposure. It indicates that  $PM_{2.5}$  reduction targeting more populous areas also lessens  $>4$  times as many premature mortality as uniform reduction does.



**Figure 7.** Frequency distribution of  $\Delta Mort$  of Hong Kong among the 804 tests. The blue-dashed line represents  $\Delta Mort$  when uniformly reducing  $PM_{2.5}$  concentration. The green-dashed line shows the mean  $\Delta Mort$  when  $PM_{2.5}$  reduction targets more populated areas.

### 4.3. The BRT Values for Districts of HK

Figure 8 shows the BRT for exposure in different districts of Hong Kong. All districts experienced a BRT value above one, underscoring their potential exposure benefits from the targeting reduction of  $PM_{2.5}$  concentration in population hotspots. The lowest BRT values (e.g., 1.32 for Yau Tsim Mong and 1.48 for Sham Shui Po) were seen in central districts. In contrast, the highest BRT values exceeded five in districts such as Tai Po (BRT = 5.28) and Islands (BRT = 5.64).

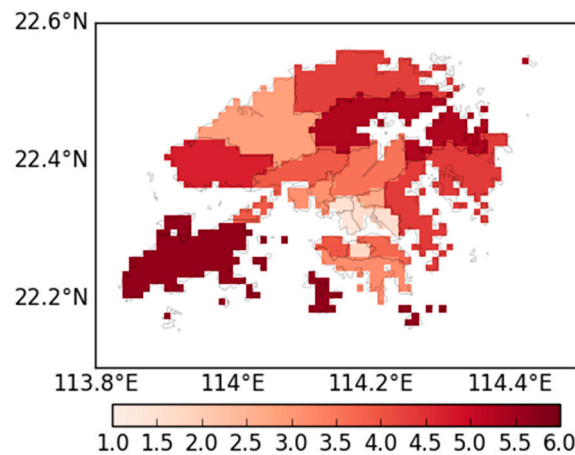


Figure 8. The BRT for exposure in different districts of Hong Kong.

Figure 9 shows relationship between the BRT value and relative standard deviation (a ratio of standard deviation and mean) of population density for eighteen districts of Hong Kong. Each blue point represents a specific district. The green square represents Hong Kong. A high coefficient of determination ( $R^2$ ) of 0.94 ( $N = 18$ ) with a slope of 1.75 and an intercept of 0.52 was found between the two variables. This high association indicates that the benefit resulting from targeting reduction becomes more substantial in regions with a greater spatial variability in population density.

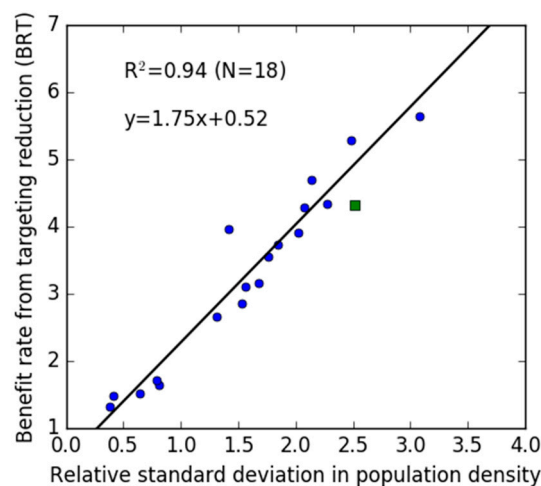


Figure 9. Relationship between the BRT value and relative standard deviation of population density for eighteen districts of Hong Kong. Each blue point represents a specific district. The green square represents Hong Kong.

## 5. Discussion

Ground observations of pollutant concentrations are sparse around the world, particularly in the low- and middle-income countries. In addition, using ground observations is difficult to explicitly assess the effect of targeting reduction because of its limited spatial coverage. Therefore, we obtained

the support from satellite remote sensing technique, which provided PM<sub>2.5</sub> data covering the entire region. To facilitate spatial matching between the pollution and population data, we used the gridded population density data instead of the census population data. The socioeconomic factors, such as the working locations, can greatly affect the human exposure level. These socioeconomic factors change greatly over time. The census provides rough socioeconomic information. More detailed and dynamic socioeconomic information can be obtained using methods such as questionnaires. In this study, the human exposure to ambient PM<sub>2.5</sub> was characterized using the available population dataset. Future studies can take into account more socioeconomic impacts if more detailed and dynamic population data are available.

The PM<sub>2.5</sub> and population data were mapped onto grids with the same spatial resolution of 0.01° × 0.01°. Within a specific grid, the distance between the locations of the two values was within 0.01° of longitude and 0.01° of latitude. To assess the uncertainties caused by this distance, we characterized the spatial variability in PM<sub>2.5</sub> concentration with an interval of one grid. For a specific grid (*i, j*), the spatial change in PM<sub>2.5</sub> concentration with one-grid interval was quantified by:  $[(PM_{i-1,j} + PM_{i+1,j} + PM_{i,j-1} + PM_{i,j+1})/4 - PM_{i,j}]/PM_{i,j}$ . Figure 10 shows spatial distribution of the one-grid PM<sub>2.5</sub> change over Hong Kong. Average absolute value of one-grid PM<sub>2.5</sub> change for all pixels over Hong Kong was estimated to be 0.93%. The grid processes of PM<sub>2.5</sub> and population data caused an uncertainty below this level.

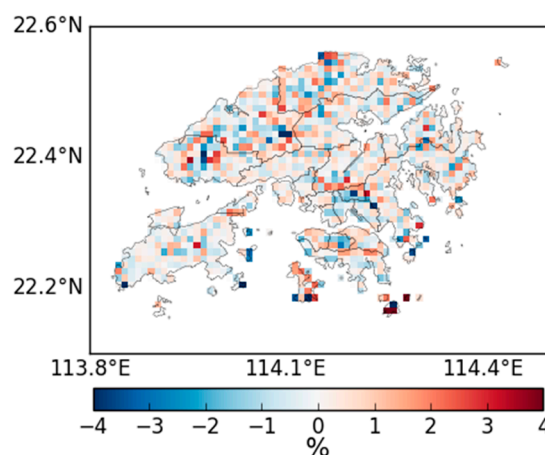


**Figure 10.** Spatial distribution of the one-grid PM<sub>2.5</sub> change over Hong Kong.

This study investigated extent of exposure and health benefits resulting from the targeting reduction of PM<sub>2.5</sub> concentration. The benefit rate of targeting reduction (i.e., the BRT values) represents a ratio of  $\Delta c_p$  with and without the targeting reduction. The use of another reduction rate (e.g.,  $-5 \mu\text{g}/\text{m}^3$ ) do not affect the benefit rate of targeting reduction (i.e., the BRT values). This study focused on investigation of the annual impact of PM<sub>2.5</sub> pollution for 2015. Emissions from various local and regional sources cause PM<sub>2.5</sub> episodes under specific synoptic conditions [38]. In 2015, daily PM<sub>2.5</sub> concentration at Tsuen Wan station (114.11°E, 22.37°N) reached  $109 \mu\text{g}/\text{m}^3$  on February 11. This level exceeded all the WHO standards for daily PM<sub>2.5</sub> concentration, including IT-1, IT-2, IT-3 and AQG. These extreme pollution events pose a strong short-term adverse impact on human health [39].

Because of the implementation of control measures, mean PM<sub>2.5</sub> concentrations over Hong Kong have experienced a decreasing trend since 2004 [40]. In addition, greater reductions of PM<sub>2.5</sub> concentrations occurred in districts in northwestern and central Hong Kong [40]. The variations in PM<sub>2.5</sub> concentrations therefore have helped Hong Kong reduce its exposure level and health burden from PM<sub>2.5</sub>. Migration of population is considered another factor that affects human exposure and health burden. Further research can be conducted to investigate these effects.

This study underscores the substantial exposure and health benefits from the targeting reduction. The potential benefits can be more significant in regions with a greater spatial variability in population

density. Taking the other cities in the PRD region as examples, great spatial variabilities in population density were seen in most of these cities [8]. As expected, the targeting reduction of  $PM_{2.5}$  concentration should also play an important role in reducing human exposure and health burden for these cities. Using the regression relationship developed in Hong Kong (shown in Figure 9), we infer the BRT values for these cities based on their population density data. Results show that the BRT levels can be as high as  $>7$  (e.g., 7.73 for Zhaoqing and 7.40 for Huizhou). Percentage bias of this projection is about 15%, estimated by the BRT value for Hong Kong (shown by the green square in Figure 9).

To better reduce exposure level and health burden, control efforts are suggested to target the population hotspots such as those in central and northwestern Hong Kong. Wu et al. [41] performed a source apportionment for  $PM_{2.5}$  for cities in the PRD region using Comprehensive Air Quality Model (CAMx) in conjunction with the Particulate Source Apportionment Technology (PSAT) module. Their results showed that  $PM_{2.5}$  in Hong Kong was determined by super-regional transport from the non-PRD region, regional transport from the PRD region and a series of local emissions. Using the same model setup (see more details in Wu et al. [41]), we update the source apportionment for  $PM_{2.5}$  for Hong Kong in 2015. The super-regional transport, regional transport and local sources contributed 68.3%, 16.9% and 14.8%, respectively, to  $PM_{2.5}$  over Hong Kong. The high impacts from super-regional and regional transports suggest the importance of super-regional and regional cooperation to reduce  $PM_{2.5}$  concentration in Hong Kong. Major local emission sources included mobile source, areas source (e.g., fuel combustion and residential emission) and marine source. Figure 11a–c) shows local-source contributions to  $PM_{2.5}$  concentration in different areas of Hong Kong at a resolution of 3 km. Figure 11d shows type of source with a maximal contribution in different areas of Hong Kong. Mobile and area sources substantially contributed to  $PM_{2.5}$  in central and northwestern Hong Kong. Marine source made a higher contribution to  $PM_{2.5}$  in coastal areas of Hong Kong. These results suggest that, to better protect public health, local environmental policy is suggested to aim at reducing anthropogenic emissions from mobile and area sources in central and northwestern areas.

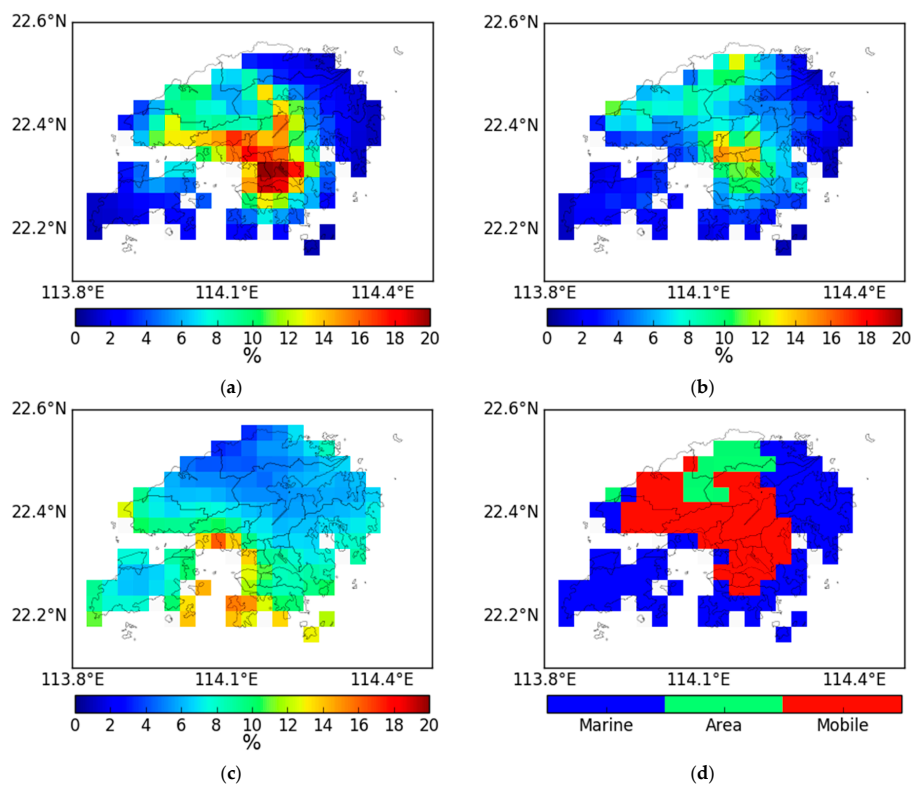


**Figure 11.** Contributions from local (a) mobile source, (b) area source and (c) marine source to  $PM_{2.5}$  in different areas of Hong Kong at a resolution of 3 km. (d) Type of source with a maximal contribution in different areas of Hong Kong.

## 6. Conclusions

Quantitative assessment of the effect of targeting reduction is limited. This study investigated the extent of exposure and health benefits resulting from the targeting reduction of PM<sub>2.5</sub> concentration. We took advantage of satellite observations to characterize spatial distribution of PM<sub>2.5</sub> concentration at a resolution of 1 km. Using Hong Kong of China as the study region (804 satellite's pixels covering its residential areas), human exposure level ( $c_p$ ) and premature mortality attributable to PM<sub>2.5</sub> ( $Mort$ ) for 2015 were estimated to be 25.9  $\mu\text{g}/\text{m}^3$  and 4112 people per year, respectively. We then performed 804 diagnostic tests that reduced PM<sub>2.5</sub> concentrations by  $-1 \mu\text{g}/\text{m}^3$  in different areas and a reference test that uniformly spread the  $-1 \mu\text{g}/\text{m}^3$ . We used a benefit rate from targeting reduction (BRT), which represented a ratio of declines in  $c_p$  (or  $Mort$ ) with and without the targeting reduction, to quantify the extent of benefits. The diagnostic tests estimated the BRT levels for both human exposure and premature mortality to be 4.3 over Hong Kong. It indicates that the declines in human exposure and premature mortality quadrupled with a targeting reduction of PM<sub>2.5</sub> concentration over Hong Kong. Our results underscore the substantial exposure and health benefits from the targeting reduction of PM<sub>2.5</sub> concentration. To better protect public health in Hong Kong, super-regional and regional cooperation are essential. Meanwhile, local environmental policy is suggested to aim at reducing anthropogenic emissions from mobile and area (e.g., residential) sources in central and northwestern areas.

**Author Contributions:** Supervision, A.K.H.L.; Writing—original draft, C.L.; Writing—review & editing, J.C.H.F., C.L., X.L., Z.L. and A.W.

**Funding:** This work was supported by the Research Grants Council of Hong Kong Government (Project No. T24/504/17), the National Natural Science Foundation of China (Grant No. 41575106), the Science and Technology Plan Project of Guangdong Province of China (Grant No. 2015A020215020), NSFC/RGC Grant N\_HKUST631/05 and the Fok Ying Tung Graduate School (NRC06/07.SC01).

**Acknowledgments:** We thank the Hong Kong Environmental Protection Department for provision of air-quality monitoring data.

**Conflicts of Interest:** The authors declare no conflict of interest. The funders had no role in the design of the study; in the collection, analyses, or interpretation of data; in the writing of the manuscript; or in the decision to publish the results.

## References

1. Crouse, D.L.; Peters, P.A.; van Donkelaar, A.; Goldberg, M.S.; Villeneuve, P.J.; Brion, O.; Khan, S.; Atari, D.O.; Jerrett, M.; Pope, C.A.; et al. Risk of nonaccidental and cardiovascular mortality in relation to long-term exposure to low concentrations of fine particulate matter: A Canadian national-level cohort study. *Environ. Health Perspect.* **2012**, *120*, 708–714. [[CrossRef](#)] [[PubMed](#)]
2. Guo, C.; Zhang, Z.; Lau, A.K.H.; Lin, C.Q.; Chuang, Y.C.; Chan, J.; Jiang, W.K.; Tam, T.; Yeoh, E.-K.; Chan, T.-C.; et al. Effect of long-term exposure to fine particulate matter on lung function decline and risk of chronic obstructive pulmonary disease in Taiwan: A longitudinal, cohort study. *Lancet Planet. Health* **2018**, *2*, e114–e125. [[CrossRef](#)]
3. Zhang, Z.; Hoek, G.; Chang, L.; Chan, T.-C.; Guo, C.; Chuang, Y.C.; Chan, J.; Lin, C.; Jiang, W.K.; Guo, Y.; et al. Particulate matter air pollution, physical activity and systemic inflammation in Taiwanese adults. *Int. J. Hyg. Environ. Health* **2018**, *221*, 41–47. [[CrossRef](#)] [[PubMed](#)]
4. Wong, C.M.; Lai, H.K.; Tsang, H.; Thach, T.Q.; Thomas, G.N.; Lam, K.B.H.; Chan, K.P.; Yang, L.; Lau, A.K.H.; Ayres, J.G.; et al. Satellite-Based Estimates of Long-Term Exposure to Fine Particles and Association with Mortality in Elderly Hong Kong Residents. *Environ. Health Perspect.* **2015**, *123*, 1167–1172. [[CrossRef](#)] [[PubMed](#)]
5. Chan, T.-C.; Zhang, Z.; Lin, B.-C.; Lin, C.; Deng, H.-B.; Chuang, Y.C.; Chan, J.W.M.; Jiang, W.K.; Tam, T.; Chang, L.; et al. Long-Term Exposure to Ambient Fine Particulate Matter and Chronic Kidney Disease: A Cohort Study. *Environ. Health Perspect.* **2018**, *126*, 107002. [[CrossRef](#)] [[PubMed](#)]

6. Zhang, Z.; Chan, T.-C.; Guo, C.; Chang, L.; Lin, C.; Chuang, Y.C.; Jiang, W.K.; Ho, K.F.; Tam, T.; Woo, K.S.; et al. Long-term exposure to ambient particulate matter (PM2.5) is associated with platelet counts in adults. *Environ. Pollut.* **2018**, *240*, 432–439. [[CrossRef](#)] [[PubMed](#)]
7. He, K.; Yang, F.; Ma, Y.; Zhang, Q.; Yao, X.; Chan, C.K.; Cadle, S.; Chan, T.; Mulawa, P. The characteristics of PM2.5 in Beijing, China. *Atmos. Environ.* **2001**, *35*, 4959–4970. [[CrossRef](#)]
8. Lin, C.Q.; Li, Y.; Lau, A.K.H.; Deng, X.J.; Tse, K.T.; Fung, J.C.H.; Li, C.C.; Li, Z.Y.; Lu, X.C.; Zhang, X.G.; et al. Estimation of long-term population exposure to PM2.5 for dense urban areas using 1-km MODIS data. *Remote Sens. Environ.* **2016**, *179*, 13–22. [[CrossRef](#)]
9. Shi, Y.; Matsunaga, T.; Yamaguchi, Y.; Li, Z.; Gu, X.; Chen, X. Long-term trends and spatial patterns of satellite-retrieved PM2.5 concentrations in South and Southeast Asia from 1999 to 2014. *Sci. Total Environ.* **2018**, *615*, 177–186. [[CrossRef](#)]
10. Van Donkelaar, A.; Martin, R.V.; Brauer, M.; Boys, B.L. Use of satellite observations for long-term exposure assessment of global concentrations of fine particulate matter. *Environ. Health Perspect.* **2015**, *123*, 135–143. [[CrossRef](#)]
11. Apte, J.S.; Marshall, J.D.; Cohen, A.J.; Brauer, M. Addressing Global Mortality from Ambient PM2.5. *Environ. Sci. Technol.* **2015**, *49*, 8057–8066. [[CrossRef](#)] [[PubMed](#)]
12. Lu, X.; Lin, C.; Li, W.; Chen, Y.; Huang, Y.; Fung, J.C.H.; Lau, A.K.H. Analysis of the adverse health effects of PM2.5 from 2001 to 2017 in China and the role of urbanization in aggravating the health burden. *Sci. Total Environ.* **2019**, *652*, 683–695. [[CrossRef](#)] [[PubMed](#)]
13. Lin, C.Q.; Lau, A.K.H.; Li, Y.; Fung, J.C.H.; Li, C.C.; Lu, X.C.; Li, Z.Y. Difference in PM2.5 variations between urban and rural areas over eastern China from 2001 to 2015. *Atmosphere* **2018**, *9*, 312. [[CrossRef](#)]
14. Washington DC World Bank. *World Bank East Asia's Changing Urban Landscape: Measuring a Decade of Spatial Growth*; World Bank: Washington, DC, USA, 2015. [[CrossRef](#)]
15. Yuan, Z.; Yadav, V.; Turner, J.R.; Louie, P.K.K.; Lau, A.K.H. Long-term trends of ambient particulate matter emission source contributions and the accountability of control strategies in Hong Kong over 1998–2008. *Atmos. Environ.* **2013**, *76*, 21–31. [[CrossRef](#)]
16. Zheng, M.; Cheng, Y.; Zeng, L.; Zhang, Y. Developing chemical signatures of particulate air pollution in the Pearl River Delta region, China. *J. Environ. Sci.* **2011**, *23*, 1143–1149. [[CrossRef](#)]
17. Lai, S.; Zou, S.; Cao, J.; Lee, S.; Ho, K. Characterizing ionic species in PM2.5 and PM10 in four Pearl River Delta cities, South China. *J. Environ. Sci.* **2007**, *19*, 939–947. [[CrossRef](#)]
18. Li, Z.; Che, W.; Frey, H.C.; Lau, A.K.H.; Lin, C. Characterization of PM2.5 exposure concentration in transport microenvironments using portable monitors. *Environ. Pollut.* **2017**, *228*, 433–442. [[CrossRef](#)]
19. Liao, Z.; Sun, J.; Liu, J.; Guo, S.; Fan, S. Long-term trends in ambient particulate matter, chemical composition, and associated health risk and mortality burden in Hong Kong (1995–2016). *Air Qual. Atmos. Health* **2018**, *11*, 773–783. [[CrossRef](#)]
20. Lu, X.; Lin, C.; Li, Y.; Yao, T.; Fung, J.C.H.; Lau, A.K.H. Assessment of health burden caused by particulate matter in southern China using high-resolution satellite observation. *Environ. Int.* **2017**, *98*, 160–170. [[CrossRef](#)]
21. Zhong, L.; Louie, P.K.K.; Zheng, J.; Yuan, Z.; Yue, D.; Ho, J.W.K.; Lau, A.K.H. Science–policy interplay: Air quality management in the Pearl River Delta region and Hong Kong. *Atmos. Environ.* **2013**, *76*, 3–10. [[CrossRef](#)]
22. Van Donkelaar, A.; Martin, R.V.; Brauer, M.; Kahn, R.; Levy, R.; Verduzco, C.; Villeneuve, P.J. Global estimates of ambient fine particulate matter concentrations from satellite-based aerosol optical depth: Development and application. *Environ. Health Perspect.* **2010**, *118*, 847–855. [[CrossRef](#)] [[PubMed](#)]
23. Li, Y.; Lin, C.; Lau, A.K.H.; Liao, C.; Zhang, Y.; Zeng, W.; Li, C.; Fung, J.C.H.; Tse, T.K.T. Assessing Long-Term Trend of Particulate Matter Pollution in the Pearl River Delta Region Using Satellite Remote Sensing. *Environ. Sci. Technol.* **2015**, *49*, 11670–11678. [[CrossRef](#)] [[PubMed](#)]
24. Liu, J.; Han, Y.; Tang, X.; Zhu, J.; Zhu, T. Estimating adult mortality attributable to PM2.5 exposure in China with assimilated PM2.5 concentrations based on a ground monitoring network. *Sci. Total Environ.* **2016**, *568*, 1253–1262. [[CrossRef](#)] [[PubMed](#)]
25. Lao, X.Q.; Zhang, Z.; Lau, A.K.; Chan, T.-C.; Chuang, Y.C.; Chan, J.; Lin, C.; Guo, C.; Jiang, W.K.; Tam, T.; et al. Exposure to ambient fine particulate matter and semen quality in Taiwan. *Occup. Environ. Med.* **2017**. [[CrossRef](#)] [[PubMed](#)]

26. Lin, C.Q.; Li, C.C.; Lau, A.K.H.; Yuan, Z.B.; Lu, X.C.; Tse, K.T.; Fung, J.C.H.; Li, Y.; Yao, T.; Su, L.; et al. Assessment of satellite-based aerosol optical depth using continuous lidar observation. *Atmos. Environ.* **2016**, *140*, 273–282. [[CrossRef](#)]
27. Zou, B.; Chen, J.; Zhai, L.; Fang, X.; Zheng, Z.; Zou, B.; Chen, J.; Zhai, L.; Fang, X.; Zheng, Z. Satellite Based Mapping of Ground PM<sub>2.5</sub> Concentration Using Generalized Additive Modeling. *Remote Sens.* **2016**, *9*, 1. [[CrossRef](#)]
28. Si, Y.; Li, S.; Chen, L.; Yu, C.; Zhu, W.; Si, Y.; Li, S.; Chen, L.; Yu, C.; Zhu, W. Estimation of Satellite-Based SO<sub>4</sub><sup>2-</sup> and NH<sub>4</sub><sup>+</sup> Composition of Ambient Fine Particulate Matter over China Using Chemical Transport Model. *Remote Sens.* **2017**, *9*, 817. [[CrossRef](#)]
29. Dobson, J.E.; Bright, E.A.; Coleman, P.R.; Durfee, R.C.; Worley, B.A. LandScan: A global population database for estimating populations at risk. *Photogramm. Eng. Remote Sens.* **2000**, *66*, 849–857.
30. Bhaduri, B.; Bright, E.; Coleman, P.; Urban, M.L. LandScan USA: A high-resolution geospatial and temporal modeling approach for population distribution and dynamics. *GeoJournal* **2007**, *69*, 103–117. [[CrossRef](#)]
31. Ghosh, T.L.; Powell, R.D.; Elvidge, C.E.; Baugh, K.C.; Sutton, P.; Anderson, S. Shedding Light on the Global Distribution of Economic Activity. *Open Geogr. J.* **2010**, *3*. [[CrossRef](#)]
32. Goldewijk, K.K.; Beusen, A.; Janssen, P. Long-term dynamic modeling of global population and built-up area in a spatially explicit way: HYDE 3.1. *Holocene* **2010**, *20*, 565–573. [[CrossRef](#)]
33. Yao, S.; Loo, B.P.Y. Safety in numbers for cyclists beyond national-level and city-level data: A study on the non-linearity of risk within the city of Hong Kong. *Int. Prev. J. Int. Soc. Child Adolesc. Inj. Prev.* **2016**, *22*, 379–385. [[CrossRef](#)] [[PubMed](#)]
34. Li, C.; Lau, A.K.H.; Mao, J.; Chu, D.A. Retrieval, validation, and application of the 1-km aerosol optical depth from MODIS measurements over Hong Kong. *IEEE Trans. Geosci. Remote Sens.* **2005**, *43*, 2650–2658. [[CrossRef](#)]
35. Lin, C.Q.; Li, Y.; Yuan, Z.B.; Lau, A.K.H.; Li, C.C.; Fung, J.C.H. Using satellite remote sensing data to estimate the high-resolution distribution of ground-level PM<sub>2.5</sub>. *Remote Sens. Environ.* **2015**, *156*, 117–128. [[CrossRef](#)]
36. Lin, C.Q.; Liu, G.; Lau, A.K.H.; Li, Y.; Li, C.C.; Fung, J.C.H.; Lao, X.Q. High-resolution satellite remote sensing of provincial PM<sub>2.5</sub> trends in China from 2001 to 2015. *Atmos. Environ.* **2018**, *180*, 110–116. [[CrossRef](#)]
37. Burnett, R.T.; Pope, C.A., III; Ezzati, M.; Olives, C.; Lim, S.S.; Mehta, S.; Shin, H.H.; Singh, G.; Hubbell, B.; Brauer, M.; et al. An Integrated Risk Function for Estimating the Global Burden of Disease Attributable to Ambient Fine Particulate Matter Exposure. *Environ. Health Perspect.* **2014**. [[CrossRef](#)] [[PubMed](#)]
38. Fung, J.C.H.; Lau, A.K.H.; Lam, J.S.L.; Yuan, Z. Observational and modeling analysis of a severe air pollution episode in western Hong Kong. *J. Geophys. Res. Atmos.* **2005**, *110*. [[CrossRef](#)]
39. Dominici, F.; Peng, R.D.; Bell, M.L.; Pham, L.; McDermott, A.; Zeger, S.L.; Samet, J.M. Fine Particulate Air Pollution and Hospital Admission for Cardiovascular and Respiratory Diseases. *JAMA* **2006**, *295*, 1127–1134. [[CrossRef](#)]
40. Lin, C.Q.; Li, Y.; Lau, A.K.H.; Li, C.C.; Fung, J.C.H. 15-Year PM<sub>2.5</sub> Trends in the Pearl River Delta Region and Hong Kong from Satellite Observation. *Aerosol. Air Qual. Res.* **2018**, *18*, 2355–2362. [[CrossRef](#)]
41. Wu, D.; Fung, J.C.H.; Yao, T.; Lau, A.K.H. A study of control policy in the Pearl River Delta region by using the particulate matter source apportionment method. *Atmos. Environ.* **2013**, *76*, 147–161. [[CrossRef](#)]

